Limnol. Oceanogr., 53(1), 2008, 172–184

Changes in phosphorus biogeochemistry along an estuarine salinity gradient: The iron conveyer belt

Thomas E. Jordan
Smithsonian Environmental Research Center, P.O. Box 28, Edgewater, Maryland 21037

Jeffrey C. Cornwell
University of Maryland Center for Environmental Science, Horn Point Laboratory, Cambridge, Maryland 21613

Walter R. Boynton and Jon T. Anderson[1]
University of Maryland Center for Environmental Science, Chesapeake Biological Laboratory, Solomons, Maryland 20688

Abstract

We used sequential extractions to quantify different forms of particulate phosphorus (PP) in sediments along the salinity gradient of the Patuxent River estuary. About 50–90% of the PP was phosphate bound to iron oxides (Fe-P), and 8–30% was organic P (org-P). Loosely sorbed phosphate (sorb-P), detrital apatite, and authigenic plus biogenic apatite each made up <10% of the PP. Suspended sediments from the watershed and deposited sediments in tidal freshwater had the highest concentrations of Fe-P, ranging about 30–55 μmol g^{-1} sediment. As pore-water salinity increased to 7 along the estuarine gradient, Fe-P declined to 15–25 μmol g^{-1}, org-P increased from 4 to 10 μmol g^{-1}, sorb-P increased from 0.5 to 2.5 μmol g^{-1}, and total sediment PP declined from 60 to 40 μmol g^{-1}. Concentrations of pore-water solutes also changed with salinity. As salinity increased, dissolved Fe and ammonium decreased, while dissolved phosphate increased. Near the freshwater end of the gradient, the molar ratio of pore-water ammonium : phosphate was generally >16 (the Redfield ratio) and ranged up to >700, while at the saline end of the gradient the ratio was generally <16 and ranged down to <1.5. Our observations are consistent with the hypothesis that phosphate is released from terrigenous sediments when they are deposited in saline portions of the estuary where sulfide may enhance dissolution of Fe-P and form Fe sulfide precipitates. Such phosphate release may contribute to the generally observed switch from phosphorus limitation in freshwater to nitrogen limitation in coastal marine water.

Driven by large-scale anthropogenic alterations of N and P cycles, eutrophication has become a major environmental problem in freshwater, estuarine, and coastal water throughout the world (e.g., Cloern 2001). Primary production is usually limited by P in freshwater and N in seawater (e.g., Howarth and Marino 2006), although there are exceptions to this paradigm. In some parts of the ocean, P or Fe may be limiting (e.g., Wu et al. 2000), and P supply may set the long-term limit on oceanic production (Tyrrell 1999). However, N supply usually sets the short-term limit on production in coastal seawater. In estuaries, where freshwater and seawater mix, spatial and temporal changes in the relative availabilities of N and P cause shifts in nutrient limitation (e.g., Fisher et al. 1999), presenting difficulties for prioritizing nutrient management.

More than 90% of the P carried by rivers to estuaries and coastal waters is associated with suspended solids (Follmi 1996). Particulate P (PP) may be bound to Fe, Mn, Al, Ca, or organic C. Often, operationally defined PP fractions are analyzed by sequential extractions and digestions (e.g., Ruttenberg 1992). Such analyses have rarely been applied to suspended particles in streams and rivers (Berner and Rao 1994; Pacini and Gächter 1999; Subramanian 2000). Moreover, riverine fluxes of total PP are poorly quantified because a large proportion of the flux of particulate matter generally occurs during brief, unpredictable episodes of high water flow that often go unobserved (Correll et al. 1999). Thus, the amount of PP entering estuaries, its chemical composition, and its eventual fate are not well known.

Much of the fluvial PP may be converted to biologically available dissolved inorganic P (DIP) in estuaries through processes that are enhanced by increasing salinity. Interactions of the Fe, S, and P cycles may have important effects on PO_4^{3-} availability along salinity gradients. More than half the fluvial PP may be bound to iron oxyhydroxides (FeOOH; Compton et al. 2000). This P can be released into solution when FeOOH is reduced in anoxic layers of sediments. When this happens under aerobic freshwater, the resulting Fe(II) can diffuse upward into aerobic

[1] Present address: Morgan State University Estuarine Research Center, St. Leonard, Maryland 20685.

Acknowledgments

Funding was provided by National Science Foundation grant DEB-0235884. Technical assistance was provided by Nancy Goff, Joseph Miklas, Nicole Mitchell, Wendy Milonovich, Marc Sigrist, Erica Kiss, Mike Owens, and Eva Bailey. Help also came from graduate students Sarah Greene, Jennifer O'Keefe, Rebecca Holyoke, and Jeanne Hartzell and Smithsonian undergraduate interns Tori Ziemann, Jessica Soule, Sheena Young, and Jenna Jandorf. Intern support was provided by National Science Foundation REU grants DBI-0097216 and DBI-0353759 and by a NOAA Sea Grant Minority Internship. Dr. Federica Tamburini provided helpful advice on SEDEX sequential extraction methods. This paper was improved by the suggestions of two anonymous reviewers.

sediments and be oxidized to FeOOH that can bind PO_4^{3-}, preventing it from diffusing into the overlying water. In contrast, sulfides formed by SO_4^{2-} reduction in the anoxic layers of sulfate-rich saltwater sediment precipitate Fe(II), preventing it from diffusing to aerobic layers where it might otherwise reoxidize and bind PO_4^{3-} (Caraco et al. 1990). Also, sulfides can promote the reduction of FeOOH in anoxic sediments (Jensen et al. 1995). The enhancement of PO_4^{3-} efflux from sediments due to sulfides could promote the general tendency of P limitation in freshwater and N limitation in saltwater (Caraco et al. 1990).

Salinity also affects the chemical form of refractory phosphorus that is eventually buried in the sediment. In freshwater, Fe and P can be buried as vivianite ($Fe_3(PO_4)_2$ 8 H_2O) or other ferrous compounds, which will not form in brackish water where Fe(II) combines with sulfides (Roden and Edmonds 1997; Gächter and Müller 2003). In saltwater, reduction of FeOOH below the oxic layer in sediments releases PO_4^{3-} and fluoride into solution, thus leading to the formation of carbonate fluorapatite, a P mineral that accumulates in marine sediments (Ruttenberg 1992; Ruttenberg and Berner 1993). Since salinity affects the form of buried P, it may also affect the rate of P burial.

Delivery of bioavailable P to the ocean is not well quantified because of uncertainties about the fate of FeOOH-bound P (Compton et al. 2000). Thus, dissolution of FeOOH-bound P in estuarine sediments may play an important role in the global P cycle. Delivery of bioavailable P to the ocean may affect other global biogeochemical cycles, such as the carbon cycle (Follmi 1996), because of the long-term limitation of ocean productivity by P supply.

Inorganic PP (PIP) may be more important than organic PP in shifting the relative availability of P and N along estuarine salinity gradients. Mineralization of organic matter releases N as well as P, and therefore the effect of mineralization on the relative abundance of N and P depends on the N : P ratio of the organic matter. In contrast, release of DIP from PIP is not accompanied by release of N. Based on analysis of N and P budgets, release of DIP from PIP in terrigenous sediments appears to be the most important mechanism decreasing the N : P ratio in the upper Rhode River estuary (Jordan et al. 1991).

We hypothesize that Fe flowing from land to sea acts as a horizontal conveyer belt carrying PO_4^{3-} through freshwater environments without releasing the PO_4^{3-} until reaching saline water. In freshwater, FeOOH-bound PO_4^{3-} may be released in anoxic conditions, but the resulting dissolved Fe(II) will remain available to reoxidize and reprecipitate the released PO_4^{3-} once encountering oxygen. Thus, the iron conveyer belt is not fully unloaded until sulfides precipitate the Fe(II).

In this study we examine a portion of the Fe conveyer belt hypothesis by investigating changes in the biogeochemistry of P as it moves from freshwater to mesohaline water along the salinity gradient of the Patuxent River estuary. We compare PP composition of suspended particles discharged from the watershed with PP composition of deposited and resuspended sediments along the gradient from freshwater to mesohaline water. We also compare pore-water concentrations of DIN, DIP, Fe, and sulfate along the salinity gradient.

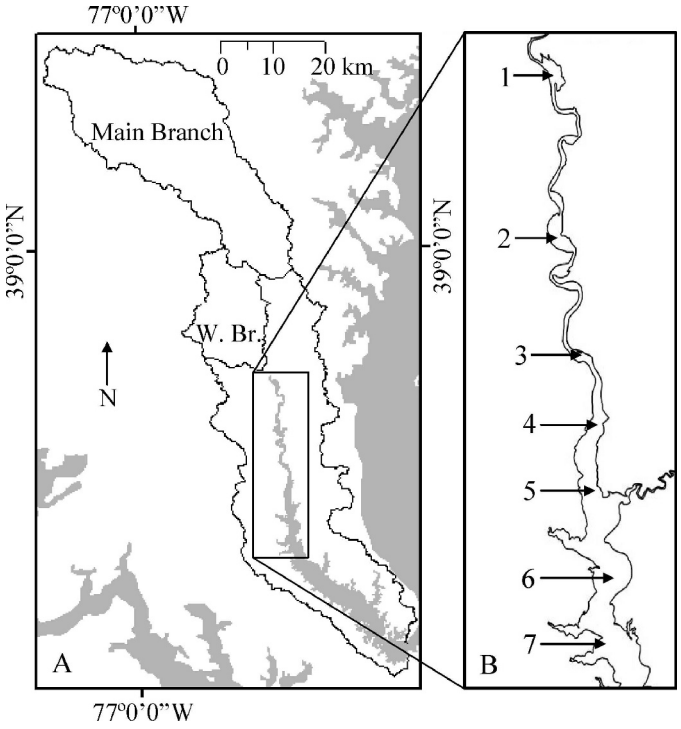

Fig. 1. (A) The Patuxent River estuary and its watershed, showing the Main Branch and Western Branch (W. Br.) watersheds monitored in this study. (B) Enlargement of the upper estuary 30–70 km from the mouth, showing the seven sampling sites.

Methods

Study site—Our study focused on the upper Patuxent River estuary from freshwater tidal to mesohaline (salinity 4–14) waters (Fig. 1; Table 1). The Patuxent River is the sixth-largest tributary estuary of Chesapeake Bay. The tidal portion of the river is about 80 km long, covers 137 km^2, and averages 5 m deep. In the lower estuary, maximum depths reach 40 m, but in the area we studied, depths are generally less than 10 m. Salinity at the mouth of the Patuxent, where it joins Chesapeake Bay, fluctuates from 8 to 18 seasonally (Lung and Bai 2003). The fresh and oligohaline waters are vertically well mixed and aerobic, but waters of the lower estuary are stratified most of the year, with a typical two-layer estuarine mixing pattern and sometimes with hypoxic conditions in the lower layer (Lung and Bai 2003). The 2,393-km^2 drainage basin of the Patuxent River is about 15% cropland, 6% pasture, 44% forest, and 35% other land types (mostly residential; Environmental Protection Agency–Environmental Monitoring and Assessment Program [EPA-EMAP] 1994). About one-third of the watershed is in the Piedmont physiographic province, and the remainder is in the Coastal Plain.

The Patuxent estuary is the subject of intensive ongoing long-term studies, including analyses of estuarine nutrient

Table 1. Total areas (km²) and percentages of land cover types (EPA-EMAP 1994) in study watersheds and major subbasins of the Patuxent River Basin. The monitored streams included the Main Branch and the Western Branch of the Patuxent River, watersheds 251.1 and 235, respectively, in Jordan et al. (2003). The Main Branch watershed includes all the Piedmont lands.

Watershed	Land area (km²)	Forest (%)	Grassland (%)	Developed (%)	Cropland (%)
Western Branch	230	37	33	23	6.9
Main Branch	900	44	29	19	7.8
Piedmont	630	42	36	13	9.5
Coastal Plain	1,600	52	25	12	10
Whole Patuxent Basin	2,300	49	28	12	10

dynamics (e.g., Fisher et al. 2006). The Chesapeake Bay Program monitors water quality throughout the estuary (Maryland Department of the Environment), and models of water quality and mixing have been produced (e.g., Lung and Bai 2003). Several studies have documented an increasing N load to the estuary from 1950 to 1985 accompanied by increases in phytoplankton biomass, decreases in water clarity, and demise of submerged aquatic vegetation (SAV) (Boynton 2000). Recent declines in N load have somewhat reversed the trends in phytoplankton and water clarity, but clarity is still too low to support SAV or benthic algae in most of the estuary (Boynton 2000).

Patterns of N and P dynamics in the Patuxent are typical of many estuaries. Strong seasonal fluctuations in DIP and NO_3^- generally cause atomic DIN : DIP ratios to shift from >40 to <4. This results in a switch in phytoplankton limitation from P in spring to N in summer (Fisher et al. 1999). DIP concentration rises to a sharp peak in late summer just downstream of the salinity front, indicating a net production of DIP in that section of the estuary. The location of the DIP peak does not correspond to a region of anoxic water or high pH (Chesapeake Bay Program data, www.eyesonthebay.net) but does correspond to the zone of greatest seasonal change in salinity.

Sampling and chemical analyses—Extending the work of Jordan et al. (2003), we used automated samplers to monitor discharge of water and to collect water samples from two streams that together drain about 49% of the Patuxent River watershed (Fig. 1; Table 1). From August 1997 to July 1999 and from November 2002 to December 2004, the samplers monitored stream depth, calculated water flow from rating curves of flow versus depth, and controlled pumps to take samples of stream water after a set amount of flow had occurred. Thus, samples were pumped more frequently at higher flow rates and accumulated as flow-weighted composites that were collected weekly for analysis.

Measured portions of the composite samples were filtered with preweighed 0.4-μm Nuclepore filters that were dried and reweighed to measure the concentration of total suspended solids (TSS). The filters plus TSS were stored dry prior to serial extractions of forms of PP.

From March 2003 to June 2005, we collected sediment cores at seven locations along the salinity gradient of the upper Patuxent River estuary, numbered from 1 at the freshwater end of the gradient to 7 at the saline end (Fig. 1). We sampled sediment at each site using either a Soutar box corer or, if water depths were <3 m, a pole corer. The 15–20-cm-long cores were collected in 6.3-cm ID clear acrylic cylinders that were inserted manually into the sediment collected in the box corer or inserted directly into the bottom sediment using the pole corer. Immediately after collection, the core tubes were stoppered and placed in containers of estuarine water to maintain ambient temperature during transport to the laboratory. In the laboratory the core tubes were opened at the top and kept submerged in containers of aerated estuarine water from their particular collection sites.

Within 2 d of collection, the cores were extruded and sectioned under N_2 in glove bags. A 15–30-mL portion of each core section was loaded into a 50-mL polyethylene centrifuge tube that was capped while in the glove bag. The sections were centrifuged at 1,800 *g* for 30 min. The supernatant pore water was then filtered with 0.45-μm polycarbonate Millipore syringe filters.

From each core section, 2 mL of filtered pore water were collected in a 7-mL polyethylene scintillation vial, acidified with 20 μL of concentrated Ultrex nitric acid, and stored for analysis of dissolved Fe. The remaining filtered pore water from each core section was collected in a 20-mL polyethylene scintillation vial. From this vial measured amounts (0.1–1 mL) were immediately transferred to two 7-mL polyethylene scintillation vials that were then brought to 5 mL with distilled water and stored frozen prior to analysis of dissolved phosphate (PO_4^{3-}) and dissolved ammonium (NH_4^+). The pore water remaining in the 20-mL vial was frozen for analysis of SO_4^{2-} and Cl^-.

After the supernatant pore water was removed, the pH of the sediment pellet was measured by inserting a Ross combination electrode. The sediment pellets were then weighed, freeze-dried, and reweighed to measure porewater inclusion in the dried portion.

Settling suspended matter was collected with sediment traps deployed monthly for 48-h periods at seven locations along the salinity gradient (Fig. 1). The sediment traps are 10-cm-diameter by 30-cm-height plastic cylinders suspended 1 m above the bottom by an anchored float. The traps were arranged in pairs mounted on a holder with fins that swiveled to keep the paired traps side by side and perpendicular to the current. Subsamples of trapped sediment were freeze-dried prior to serial extractions of P fractions.

Five operationally defined forms of particulate P were extracted sequentially by the SEDEX method (Ruttenberg 1992). The sequence of extractants and their targeted P forms were as follows: 1 mol L^{-1} $MgCl_2$ for loosely sorbed P (sorb-P), citrate-dithionite-bicarbonate (CDB) solution

for ferric Fe-bound P (Fe-P), pH 4 acetate-acetic acid solution for authigenic carbonate fluorapatite P plus biogenic hydroxyapatite P plus calcium carbonate bound P (auth-P), 1 mol L^{-1} HCl for detrital apatite P (det-P), and 2 mol L^{-1} HCl after ashing residual material for organic P (org-P). Although the extractions may dissolve nontargeted PP forms, we will refer to the extracts by abbreviations of their targeted PP form.

The first four extractions were done in sealed 250-mL polycarbonate filter funnels (Nalgene DS0310-4000) holding 0.2-μm Nuclepore filters. Either a weighed sample of about 0.4 g of freeze-dried ground sediment or a 0.4-μm Nuclepore filter with <0.4 g of adhering TSS was shaken in each filter funnel with 40 mL of extractant or rinse solution. The extractions followed Ruttenberg (1992) with minor modifications suggested by F. Tamburini (pers. comm.). The modifications included using two $MgCl_2$ extractions and one water rinse for sorb-P and shaking CDB and acetate extractions for 5 h each. For the CDB extraction, 0.92 g of dry sodium dithionite was added to the filter funnel, and then 40 mL of citrate bicarbonate solution were added to produce the CDB extractant in the funnel. After the specified extraction time, the extractant or rinse was vacuum filtered from the filter funnel, collected for analysis, and replaced by the next extractant or rinse in the sequence. While being shaken, the stems of the filter funnels were fitted with a 5-cm length of Tygon tubing plugged by either a rubber stopper or a stopcock to prevent loss of usually <10 mL of extractant that drained through the filter during shaking.

For the fifth and last P fraction in the series (org-P), the residual solids in the filter funnel along with the filter were transferred to a 20-mL glass vial. Then 4 mL of 50% $Mg(NO_3)_2$ were added, and the contents of the vial were dried at 60°C and later combusted at 550°C for 2 h. After combustion, 10 ml of 2 mol L^{-1} HCl were added to the ash and shaken for 24 h to extract P.

Dissolved orthophosphate (PO_4^{3-}) was analyzed in filtered pore water and in extractants (except CDB) by reaction with salicylate and hypochlorite in nitroferricyanide (Parsons et al. 1984). For pore-water PO_4^{3-}, the color development reaction was carried out in the vial used to store the prediluted sample. This ensured that any PO_4^{3-} that precipitated with Fe(III) during storage would be redissolved during the analysis rather than being lost on the walls of the storage vial.

Total P, Fe, Mn, and Al were analyzed in CDB extracts using a Perkin Elmer ICP-OES model 3000 spectrometer. Dissolved ammonium (NH_4^+) in pore water was analyzed with an Astoria Pacific automated analyzer (Method A303-S02). Dissolved Fe in pore water was analyzed by atomic absorption spectrophotometry. Sulfate (SO_4^{-}) and chloride (Cl^-) in pore water were analyzed using a Dionex model 4000 ion chromatograph. Total N and C in dried sediments were analyzed with a Perkin Elmer Model 2400 Series II CHNS/O Analyzer.

Results

PP forms in TSS discharged from the watershed—As the concentration of TSS in stream water increased, there were decreases in the concentrations of sorb-P, Fe-P, and auth-P on the TSS (Fig. 2). These relationships between TSS and PP concentrations can be described as power functions. Linear regressions of the log-transformed concentrations were statistically significant except for Fe-P from the Main Branch watershed. For PP concentrations that varied significantly with TSS concentration, we calculated the discharge-weighted mean PP concentration on the basis of the discharge of TSS from the watershed as follows. First, PP concentration was predicted from measured TSS

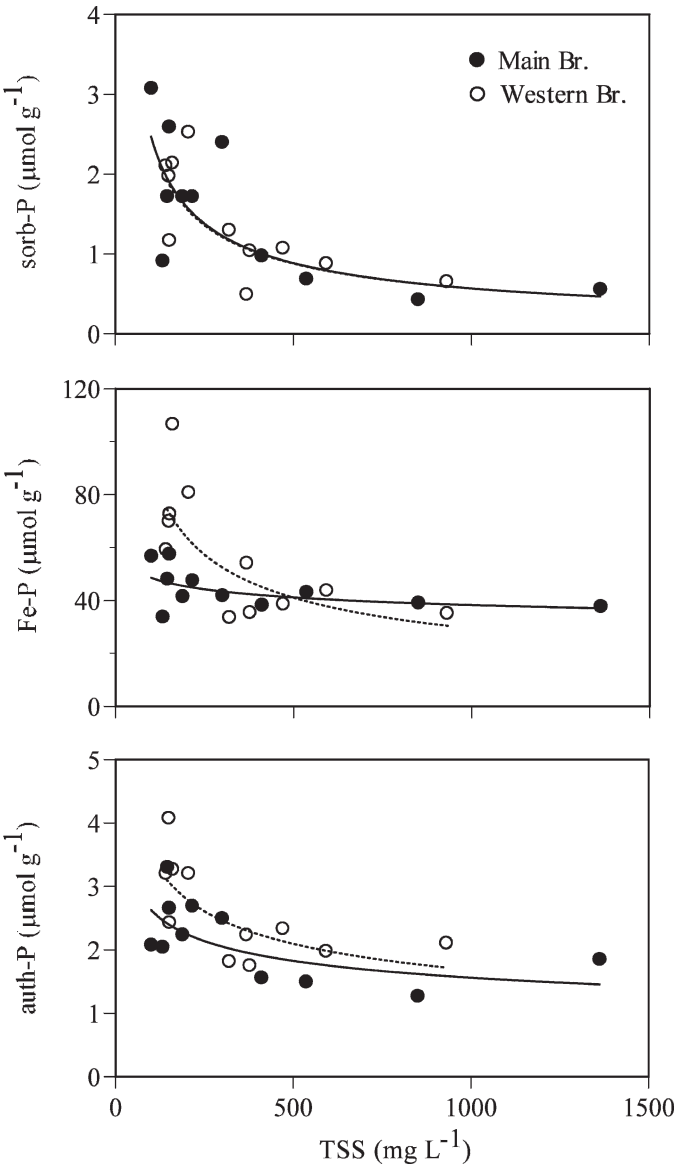

Fig. 2. Concentrations (μmol g^{-1} dry TSS) of sorb-P, Fe-P, and auth-P on total suspended solids (TSS) discharged by the Main Branch and Western Branch watersheds. Solid lines (Main Branch) and dotted lines (Western Branch) are regression fit power functions, which are all statistically significant ($p \leq 0.05$) except for Fe-P from the Main Branch watershed. Regression r^2 = 0.65 and 0.43 for sorb-P and auth-P, respectively, for Main Branch and r^2 = 0.58, 0.60, and 0.52 for sorb-P, Fe-P, and auth-P, respectively, for Western Branch.

Table 2. Mean concentrations of particulate phosphorus (PP) forms in total suspended solids (TSS) discharged from watersheds. Concentrations of sorb-P and auth-P for both watersheds and Fe-P for Western Branch are calculated as TSS discharge-weighted means. Others are arithmetic means of PP concentration measurements ± standard error ($n = 11$). Total is the sum of the tabulated values.

	Western Branch (235)		Main Branch (251.1)	
PP form	Mean (μmol P g^{-1} TSS)	Percentage of total	Mean (μmol P g^{-1} TSS)	Percentage of total
sorb-P	1.39	2.0	2.82	4.7
Fe-P	55.3	80	43.9±2.3	73
auth-P	2.58	3.7	2.66	4.5
det-P	1.44±0.10	2.1	0.688±0.060	1.2
org-P	8.16±0.68	12	9.70±0.57	16
Total	68.9	100	59.8	100

concentration on the basis of the log-log regressions of PP concentration versus TSS concentration, correcting for bias from log transformation (Sprugel 1983). Then the total watershed discharges of TSS and the PP forms were calculated by multiplying the measured water flow by the measured or predicted concentrations. Discharges of TSS and PP forms were summed for all available weekly measurements of water flow and TSS concentration in flow-weighted composite samples collected during the present study (November 2002–December 2004) and during the Jordan et al. (2003) study (August 1997–July 1999). Finally, the sum of the PP discharge was divided by the sum of the TSS discharge to obtain the discharge-weighted mean PP concentration on the TSS particles (μmol P g^{-1} TSS). These discharge-weighted means represent the average composition of TSS delivered to the estuary from the watershed.

The proportions of different PP forms in TSS differed greatly. The most abundant PP form was Fe-P, which made up 80% and 73% of the total PP in TSS from the Western Branch and Main Branch watersheds, respectively (Table 2). The next most abundant PP form was org-P, which made up 12% and 16% of the total PP in TSS from the Western Branch and Main Branch watersheds, respectively (Table 2). All other PP forms individually made up <5% of the total PP (Table 2).

PP forms in estuarine sediments along the salinity gradient—The concentration of Cl^- in pore water defines the salinity gradient we studied. Pore-water salinity, calculated from Cl^-, ranged from near 0 at the freshwater end to about 6 at the saline end at depths of 0–0.25 cm in the sediment (Fig. 3). Pore-water salinity increased with depth in the sediments, averaging up to about 7.5 at depths of 9–11 cm at the saline end of the gradient (Fig. 3).

As in TSS from the watersheds, Fe-P was the most abundant PP form and org-P the second most abundant in deposited sediments and in sediments collected by sediment traps. However, the concentration of PP forms varied with depth in the sediment and position along the salinity gradient. Fe-P, sorb-P, and total PP decreased in concentration with increasing depth in the sediment, while depth patterns were unclear for other forms of PP (Fig. 4). The depth trends for Fe-P and total PP were reflected in material collected by sediment traps, consisting mostly of mobile surface sediments resuspended by tidal currents and redeposited during slack tides (J. T. Anderson unpubl. data). However, sediment trap material had less sorb-P than did shallow deposited sediment, possibly indicating release of loosely sorbed P during resuspension.

Most important for our study are the trends along the salinity gradient. Fe-P generally decreased in concentration with increasing salinity, while sorb-P and org-P increased with increasing salinity (Fig. 4). Despite the opposing salinity-related trends, there is an overall decline in total PP as salinity increases. Salinity-related trends were not clear for apatite P forms, but det-P was lowest at the freshwater end of the gradient. Fe-P and total PP were also lower at this site than at the next site away from the freshwater end (Fig. 4). This difference runs counter to the general decrease in Fe-P and total PP concentrations with increasing salinity. However, the percentage of Fe-P in total PP was similar the two freshest sites (Fig. 5). The percentage of Fe-P decreased with increasing salinity, ranging from >80% at the freshwater end of the gradient to <50% at the saline of the gradient, while the percentage of org-P in total PP increased with increasing salinity, ranging from <10% at the freshwater end to >30% at the saltwater end (Fig. 5).

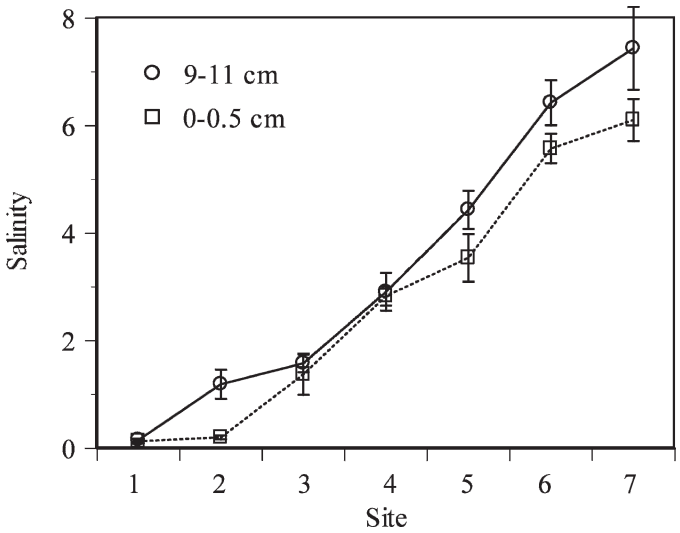

Fig. 3. Average pore-water salinity at 0–0.5-cm and 9–11-cm sampling sites 1–7. Bars with brackets are ± standard error (SE).

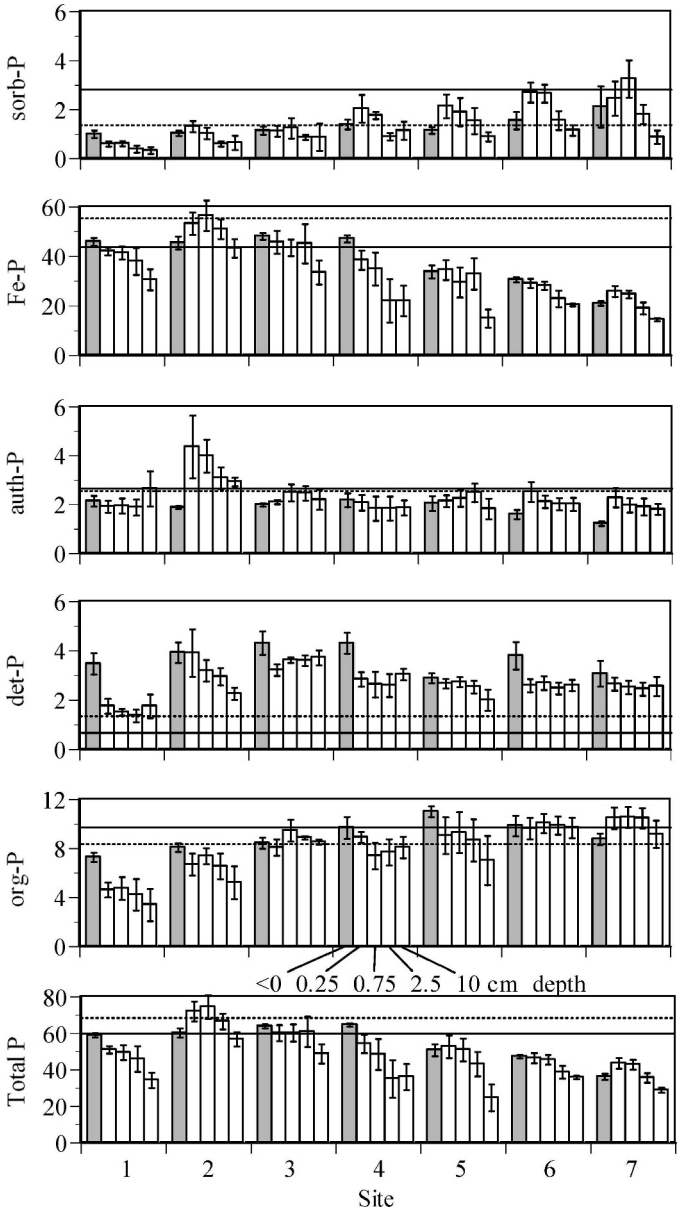

Fig. 4. Concentrations of different forms of particulate P (μmol P g^{-1} dry sediment) at various depths at sites 1–7. Gray bars labeled as <0-cm depth are samples of resuspended sediments collected with sediment traps. Bars with brackets show ± standard error (SE) for averages of four to seven samples. The horizontal solid lines (Main Branch) and dotted lines (Western Branch) show means for suspended sediments discharged from the watershed.

Extractions of Fe-P—The concentrations of Fe in the CDB extractions were consistent with the assumption that CDB extracted primarily P bound to FeOOH. Fe concentration increased with increasing P concentration in the CDB extracts, but the Fe : P ratio increased with salinity along the gradient and with depth in the sediment at some sites (Fig. 6). The atomic Fe : P ratio ranged from 7 to 9 in sediment at the freshwater end of the gradient up to about 22 at the deepest depth sampled at the most saline

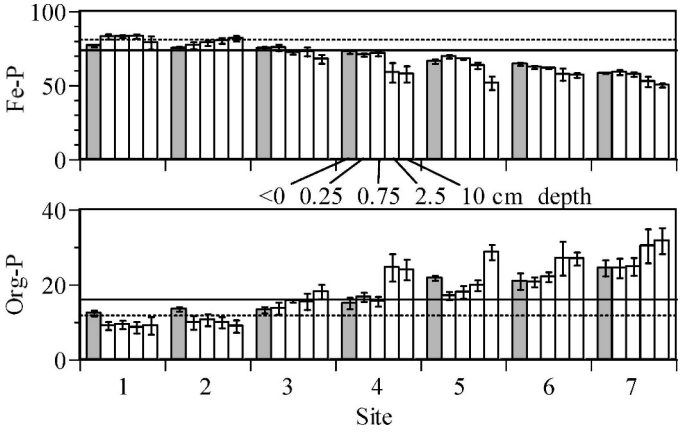

Fig. 5. Percentages of Fe-P and org-P (percentage of total P) at various depths at sites 1–7. Gray bars labeled as <0-cm depth are samples of resuspended sediments collected with sediment traps. Bars with brackets show ± standard error (SE) for averages of four to seven samples. The horizontal solid lines (Main Branch) and dotted lines (Western Branch) show means for suspended sediments discharged from the watershed.

site (Fig. 6). The changes in the Fe : P ratio with position along the salinity gradient and depth reflect mainly the spatial patterns of Fe-P because CDB-extractable Fe was less variable than Fe-P. Like Fe-P, CDB-extractable Fe concentration was lower at site 1 than at site 2, suggesting that the lower Fe-P concentration at site 1 was due to the lower FeOOH concentration there. CDB-extractable Fe, Mn, and Al were correlated and therefore showed similar relationships to P. However, the relatively low concentrations of Mn, Al, and Ca (usually <30, <50, and <20 μmol g^{-1}, respectively) in CDB extracts suggest that little of the CDB-extractable P was bound to these elements compared to the amount bound to Fe.

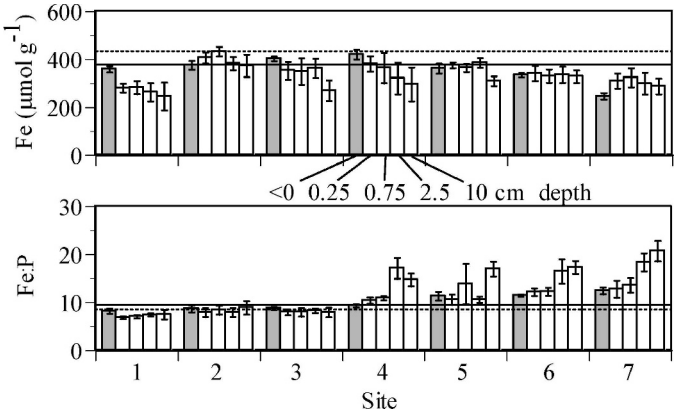

Fig. 6. Citrate-dithionite-bicarbonate (CDB)-extractable Fe (μmol g^{-1}) and the atomic ratio of CDB-extractable Fe : P at various depths at sites 1–7. Gray bars labeled as <0-cm depth are samples of resuspended sediments collected with sediment traps. Bars with brackets show ± standard error (SE) for averages of four to seven samples. The horizontal solid lines (Main Branch) and dotted lines (Western Branch) show means for suspended sediments discharged from the watershed.

Total N and organic C versus org-P—The concentrations of total N and C in the sediments are consistent with those of org-P. In freshwater sediments (collected at sites 1 and 2 in cores or sediment traps), C correlated with org-P with an atomic C : org-P ratio of about 550. In more saline sediments (sites 5, 6, and 7), there was no clear correlation between C and org-P, but this may reflect the relatively narrow range of C variation there, 2–4%, compared to 0.7–6% in freshwater sediments. The atomic C : org-P ratio averaged about 270 in sediments at sites 5, 6, and 7. Sites 3 and 4 had intermediate ratios, averaging about 450. These C : P ratios are all much higher than the Redfield C : P ratio expected for phytoplankton (106). The difference may reflect more rapid mineralization of P relative to C, or it may reflect the presence of organic matter derived from more C-rich vascular plant detritus. The increase in C : P with decreasing salinity may reflect an increase in proportions of organic C derived from vascular plant detritus closer to the source of watershed inputs and closer to the extensive tidal marshes at the head of the estuary. By comparison, the C : N atomic ratio declines from 14 in freshwater sediments to 9.2 at the most saline sites, remaining above the Redfield ratio of 6.6 and showing the same trend as C : P ratios. Similarly, total N : org-P ratios decline from 41 to 28 with increasing salinity.

Pore-water solutes—Because of the strong temporal variability of pore-water solute concentrations, we compared sites that were sampled simultaneously to investigate spatial variability. Sites 1, 2, 5, and 6 were sampled synoptically most frequently. We averaged concentrations measured at these sites on eight common dates to illustrate spatial variability of pore-water solutes.

There were clear patterns in concentrations with depth and position along the salinity gradient. Pore-water Fe concentration was highest at the freshwater end site and declined toward the saline end of the gradient. Fe concentration generally increased with depth in the sediment, but at sites 1, 5, and 6, pore-water Fe concentrations declined slightly with increasing depth below 3 cm. Unlike Fe, pore-water PO_4^{3-} was higher at the more saline sites, 5 and 6, than at the fresher sites, 1 and 2 (Fig. 7). At sites 1 and 2, pore-water PO_4^{3-} concentrations declined with increasing depth below 3 cm, but at the more saline sites, PO_4^{3-} concentrations increased steadily with depth. Pore-water PO_4^{3-} in the 1–2 mL of pore water left in samples dried for SEDEX analysis would contribute <10% of the total sorb-P we measured. Pore-water NH_4^+ was highest at sites 1 and 2 (Fig. 7). SO_4^{2-} concentrations were much higher at sites 5 and 6 than at sites 1 and 2. SO_4^{2-} depletion was calculated by comparing observed SO_4^{2-} concentration to that predicted from mixing stream water with ocean water to produce the observed Cl^- concentration. SO_4^{2-} depletion was similar at sites 2, 5, and 6 and lower at site 1 (Fig. 7). The increase SO_4^{2-} depletion with depth reflects the increase in Cl^- with depth (Fig. 3) as well as the slight decrease in SO_4^{2-} concentration with depth. Pore-water pH had less pronounced spatial patterns than other constituents. pH generally ranged from 7 near the surface to 7.4 at about 10 cm in the saline sites and from 7.0 to 7.2 at the freshwater sites.

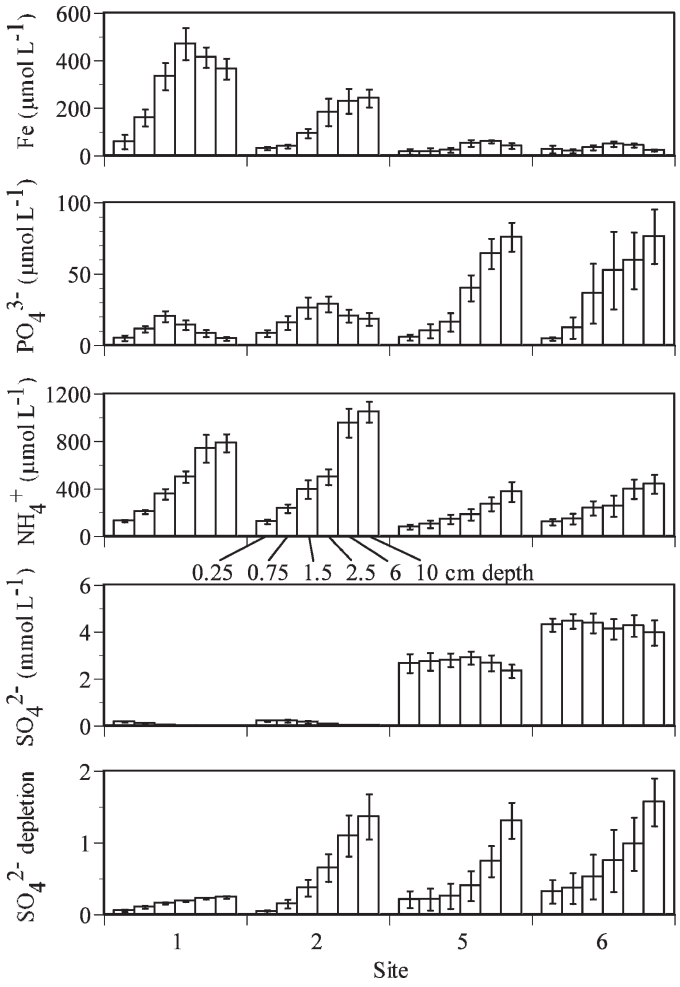

Fig. 7. Pore-water solute concentrations averaged over eight common dates at different depths at sites 1, 2, 5, and 6. Bars with brackets show averages ± standard error (SE). SO_4^{2-} depletion (mmol L^{-1}) was calculated by subtracting the measured SO_4^{2-} concentration from that predicted from mixing stream water with ocean water to produce the observed Cl^- concentration.

Because pore-water NH_4^+ and PO_4^{3-} showed contrasting patterns of variation along the salinity gradient, the $NH_4^+ : PO_4^{3-}$ ratio differed dramatically with salinity. At the two sites nearest the freshwater end of the gradient, NH_4^+ ranged up to about 2,300 μmol L^{-1}, while PO_4^{3-} concentrations generally remained below 40 μmol L^{-1} (Fig. 8). Therefore, the $NH_4^+ : PO_4^{3-}$ ratio at these sites was generally >16 (the Redfield ratio) and reached values >700. In contrast, at more saline sites, NH_4^+ generally remained below 1,000 μmol L^{-1}, while PO_4^{3-} concentrations ranged up to about 230 μmol L^{-1}. Therefore, the $NH_4^+ : PO_4^{3-}$ ratio at the saline sites was generally <16 with extreme values <1.5.

Discussion

PP forms in TSS discharged from the watershed—The decreases in concentrations of TSS-bound sorb-P, Fe-P,

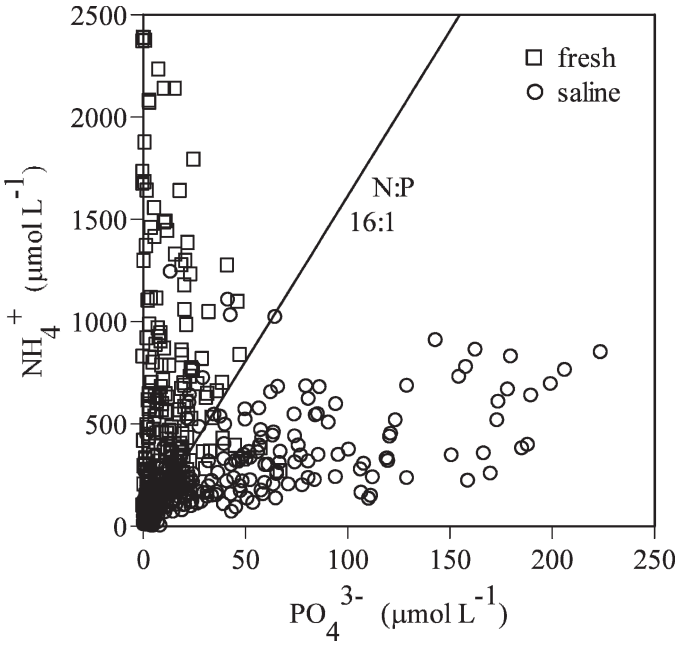

Fig. 8. Pore-water NH_4^+ versus PO_4^{3-} concentrations (μmol L^{-1}) at freshwater sites (1 and 2) and more saline sites (3–7). The line shows the 16 : 1 atomic N : P ratio.

and auth-P with increasing TSS concentration (Fig. 2) are consistent with the PP forms being bound in surface coatings on the TSS particles. Increases in the TSS concentration are associated with increasing flow and turbulence in the streams. As turbulence increases, larger particles can be held in suspension. As particle size increases, the surface area per mass of TSS decreases. Therefore, the concentrations of surface coatings per mass of particles also decrease as the size of the particles increases.

Because there have been few attempts to quantify the different fractions of PP in watershed discharges, it is not clear how much of the fluvial PP can be converted to DIP in estuaries. We found that over 94% of the total PP in watershed discharges was in nonapatite forms (Table 2) that could potentially become available P after deposition and diagenesis. However, much nonapatite P remained in the sediment at depths up to 11 cm (Fig. 4) and could become permanently buried. Other studies have found that a large proportion of riverine PP could be converted to biologically available DIP. Pionke and Kunishi (1992) found that 42% of suspended PP in agricultural watershed discharge is biologically available (readily exchangeable). Pacini and Gächter (1999) measured speciation of suspended stream-water PP at different times during rain events and found that 25–70% of the suspended PP was in nonapatite forms that may become available P after early diagenesis in lake sediments. Chambers et al. (1995) found that suspended particles from streams released DIP when exposed to sulfide, which reduced the FeOOH, thereby releasing Fe-bound P. They estimated that release of PO_4^{3-} from FeOOH in sulfide-rich sediment could account for 12.5% of the benthic P flux in the Tomales Bay estuary (Chambers et al. 1995).

The proportion of fluvial PP that can be converted to DIP is likely to vary geographically, as does the composition of fluvial PP. For example, South Asian rivers discharge PP that is generally >50% apatite, <25% Fe bound, and <10% organic (Subramanian 2000). In contrast, PP discharged from the Amazon is about equally distributed among Ca, Fe, and organic forms (Berner and Rao 1994). We found that suspended sediments discharged from the Patuxent River watershed were richer in P and Fe-P than those cited above. Previously, we found that suspended sediments discharged by Coastal Plain watersheds were richer in P than those discharged from Piedmont watersheds of Chesapeake Bay (Jordan et al. 2003). Such differences in PP composition could account for the differences in PP discharged from the entirely Coastal Plain Western Branch watershed and the partly Piedmont Main Branch watershed (Table 2).

PP forms in estuarine sediments—PP in TSS discharged from the watershed may become altered after deposition in the estuary. Concentration patterns suggest that PP deposited in freshwater retains its Fe-P, while PP deposited in saline sediments loses Fe-P after deposition (Figs. 4, 5). Fe-P concentration in Main Branch TSS was similar to that in deposited sediments at sites 1–3 but higher than that in more saline sediments. Fe-P in Western Branch TSS was somewhat elevated above that in the deposited freshwater sediment (Fig. 4), but this may reflect preferential deposition of larger-sized particles with lower Fe-P concentration. Decrease in Fe-P concentration with increasing particle size was suggested by the decrease in Fe-P in Western Branch TSS with increasing water flow (Fig. 2). Similarly, preferential settlement of larger particles may account for sorb-P and auth-P being higher in TSS than in deposited sediment (Figs. 2, 4).

The relation between org-P in TSS and deposited sediments is unclear. Concentrations of org-P in TSS are more similar to those in saline sediments than in those in freshwater sediments (Fig. 4). It is possible that the org-P in TSS is lost soon after deposition and that most of the org-P in sediment is produced within the estuary rather than imported on TSS from the watershed. Autochthonous production of org-P seems reasonable given the eutrophic status of the estuary (Fisher et al. 2006) and the abundant marshlands fringing our study area down to site 4. The high C : P ratio in sediments suggests that some of the organic matter may derive from vascular plants.

Det-P is inexplicably lower in TSS than in deposited sediments (Fig. 4). Det-P is considered very refractory in sediments (e.g., Tamburini et al. 2002), and therefore det-P concentrations should be similar in TSS and deposited sediments. The discrepancy is probably not an effect of particle size because det-P in TSS did not vary with flow rate. The det-P fraction is such a small proportion of the total PP (<10%) that inclusion of P from some source other than detrital apatite might have elevated the concentration in the det-P extractions of sediments.

Compared to other marine and estuarine sediments, the deposited sediments in the Patuxent River estuary are exceptionally rich in total P and Fe-P and include an exceptionally high proportion of Fe-P in the total SEDEX P. However, it should be noted that few studies of estuarine PP include sediments in freshwater, where we observed the highest Fe-P and PP concentrations. High Fe-P concentrations (>10 μmol g^{-1}) have also been found at sites in the northern Baltic Sea (Virtasalo et al. 2005), in the Gulf of St. Lawrence (Louchouarn et al. 1997), and in the Sacramento–San Joaquin Delta (Nilsen and Delaney 2005). In contrast, an absence of Fe-P was reported at a site in Long Island Sound and attributed to complete reduction of Fe(III) by high concentrations of sulfides (Berner et al. 1993). The majority of SEDEX P consisted of det-P in the Bohai and Yellow Seas (Liu et al. 2004), org-P at a site in the southwestern Sea of Japan (Cha et al. 2005), and auth-P in the equatorial Pacific (Filippelli and Delaney 1996; Faul et al. 2005).

Some forms of PP could be missed by the SEDEX analysis. Any organic P dissolved by extractions for sorb-P, auth-P, and det-P would not be measured by the subsequent analyses of PO_4^{3-} in the extract. In contrast, organic P dissolved by the CDB extraction for Fe-P would be included the subsequent ICP analysis of total P in the extract. This could inflate the estimate of Fe-P. Despite these potential problems, SEDEX continues to be widely used.

The Fe : P ratio in our CDB extracts is consistent with the assumption that most of the extracted P was bound to Fe. The atomic Fe : P ratios in our CDB extracts, about 7–22 (Fig. 6), are comparable to ratios found in other marine and estuarine systems, such as 6–8 in Aarhus Bay, 10–16 in the Kattegat, 17 in the Skagerrak (Jensen and Thamdrup 1993), 6–25 in the northeastern Atlantic (Van der Zee et al. 2002), and 10–12 in the Sea of Japan (Cha et al. 2005). Some studies suggest that the lower limit of Fe : P ratios may be 2 because of the formation of Fe dimers during the oxidation of Fe(II) and precipitation of the resulting Fe(III) (e.g., Virtasalo et al. 2005). However, ascorbate extractions of estuarine sediments suggest that even lower Fe : P ratios may be possible for solid Fe-P compounds (Hyacinthe and Van Cappellen 2004). Higher Fe : P ratios may indicate higher crystalinity of the Fe(III) resulting in less capacity to bind P (Van der Zee et al. 2002). We found a trend of increasing Fe : P with increasing salinity and with increasing depth in the more saline sediments (Fig. 6). This may indicate a preferential loss of less crystalline Fe(III) during early diagenesis as sediment moves toward higher salinity along the salinity gradient and is buried to deeper depths. The Fe : P trend might also be caused by CDB dissolving Fe sulfides (Slomp et al. 1996) that lack bound P and become more abundant with increasing salinity.

PP trends along the salinity gradient—Few studies have examined the changes in PP forms along estuarine salinity gradients, but others have found patterns similar to what we observed in the Patuxent. For example, in the Pamlico River estuary, concentrations of acid-extractable PO_4^{3-} and oxalate-extractable Fe in sediments decreased as salinity increased from 0 to 15, suggesting that Fe-bound P decreased with increasing salinity (Upchurch et al. 1974). Similarly, in the Delaware River estuary, Fe-P in sediments decreased from 10 μmol g^{-1} to 0.2 μmol g^{-1} along a salinity gradient from 1.8 to 29 (Strom and Biggs 1982). Decreasing concentrations of Fe-P with increasing salinity have also been found for intertidal sediments in the Cooper River (Paludan and Morris 1999) and the Scheldt (Hyacinthe and Van Cappellen 2004) and Mondego (Coelho et al. 2004) estuaries.

The decline in Fe-P with increasing salinity (Fig. 4) could be due to an increase in sulfide production with increasing salinity. Sulfides enhance the reduction of Fe(III) to Fe(II) releasing FeOOH-bound PO_4^{3-} into solution. Fe(III) reduction yields more energy to microbes than does SO_4^{2-} reduction, so SO_4^{2-} reduction is inhibited in the presence of Fe(III). However, solid Fe(III) can become coated with Fe(II) and thereby shielded from Fe-reducing bacteria (Hyacinthe and Van Cappellen 2004). Thus, Fe(III) could persist and continue to bind PO_4^{3-} even in anoxic sediments. Sulfides may remove Fe(II) coatings, exposing more Fe(III) to reduction and thereby releasing more FeOOH-bound PO_4^{3-} into solution (Weston et al. 2006). Also, Fe(III) reduction can be coupled to sulfide oxidation to SO_4^{2-} (Jensen et al. 1995). Sulfides also precipitate Fe(II), preventing it from diffusing into aerobic zones where it could reoxidize and regenerate Fe-P (Caraco et al. 1990).

Sulfides also affect the chemical form of PP that is buried in the sediment. Where sulfide is present, Fe(II) will precipitate as sulfides instead of forming ferrous phosphate compounds such as vivianite ($Fe_3(PO_4)_2$ 8 H_2O), which can accumulate in freshwater sediments (Roden and Edmonds 1997; Gächter and Müller 2003). Ferrous phosphate compounds could be dissolved by CDB and contribute to the Fe-P we measured in freshwater sediments. Formation of solid ferrous compounds may account for our observation that pore-water Fe in freshwater sediments declined in concentration with depth below 5 cm (Fig. 7).

Ionic strength also may play a role in the effect of salinity on Fe-P. Experiments with wetland peat sediments have shown that increasing salinity without adding SO_4^{-} can reduce the adsorption of PO_4^{3-} because of ion competition for adsorption sites (Beltman et al. 2000). However, we found that sorb-P increased as salinity increased (Fig. 4), but this may reflect the concurrent increase in dissolved pore-water PO_4^{3-} (Fig. 7) rather than a change in sorption capacity.

pH can also play a role in PP trends along salinity gradients. Salinity effects on DIP release from sediments may be mediated by pH because of differences between the buffering capacities of fresh and saline waters and because of increases in pH associated with SO_4^{2-} reduction in saline water (Caraco et al. 1990). An increase in pH with increasing salinity may decrease the adsorption of PO_4^{3-} to FeOOH by changing the charge of the phosphate ion (Coelho et al. 2004). Rise in pH with increasing salinity can also cause calcite precipitation, which may scavenge PO_4^{3-} from solution (De Jonge and Villerius 1989). In contrast, increases in pH to >9.5 due to high photosynthesis in

poorly buffered tidal freshwater of the Potomac (Seitzinger 1991) and Delaware (Lebo and Sharp 1993) estuaries have apparently led to releases of PO_4^{3-} from sediments. Likewise, differences in pH can account for differences in P sorption among freshwater, brackish, and saltwater tidal marsh sediments (Sundareshwar and Morris 1999). In our study sites, pore-water pH did not change greatly with salinity, ranging from 7.0 to 7.2 at the freshwater sites and from 7 to 7.4 at the saline sites, so pH differences probably do not account for the trends with salinity that we observed.

It is not clear why org-P should increase with increasing salinity in the Patuxent estuary, but the effect was to partly offset the decrease in Fe-P with increasing salinity (Fig. 4). In the Patuxent, production of org-P by phytoplankton and marsh plants may recapture P released from Fe-P, causing a switching of the sedimentary P sink from Fe-P to org-P. We found no evidence of sink switching from Fe-P to auth-P as found in the North Atlantic (Slomp et al. 1996). Our data also contrast the sink switching from org-P to auth-P found in the Mississippi Delta (Berner et al. 1993). The auth-P we measured may consist of biogenic hydroxyapatite– or calcium carbonate–bound P rather than authigenic fluorapatite, which is often a P sink in marine sediments.

Pore-water solutes—We found clear spatial trends in concentrations of pore-water solutes. Dissolved Fe decreased and dissolved PO_4^{3-} increased as salinity increased (Fig. 7), suggesting that increases in sulfide availability with increasing salinity may lead to dissolution of Fe-P and precipitation of Fe sulfides. The trend was most pronounced at depths below 5 cm in the sediment, where the atomic dissolved Fe : P ratio shifted from >10 at fresh-oligohaline sites to <1 at mesohaline sites (Fig. 7). Blomqvist et al. (2004) found similar patterns in anoxic bottom waters with ratios of dissolved Fe : P >2 in freshwater lakes and <2 in saline waters. Lehtoranta and Heiskanen (2003) found that sediments under oxic water with pore-water Fe : P >2 released PO_4^{3-} at a lower rates than sediments with pore-water Fe : P <2. They suggest that a dissolved Fe : P ratio of at least 2 is needed to provide sufficient Fe to block PO_4^{3-} efflux by forming precipitates of FeOOH-bound P in oxic surface sediments. At our sites 1 and 2, the decline in pore-water Fe concentration near the surface may be due to the precipitation of FeOOH as well as Fe efflux from the sediment. The decline in dissolved Fe with depth below 5 cm at site 1 may reflect precipitation of ferrous compounds, such as ferrous hydroxide and ferrous phosphate. Precipitation of ferrous phosphate or adsorption of PO_4^{3-} to ferrous hydroxides (Gächter and Müller 2003) could account for the decline in pore-water PO_4^{3-} concentration below 2 cm at our freshwater site.

We found that pore-water NH_4^+ concentration declined as salinity increased (Fig. 7). This may reflect the parallel decrease in DIN concentration in overlying water as salinity increased. The opposing trends of pore-water PO_4^{3-} and NH_4^+ concentrations lead to a dramatic shift in the dissolved inorganic N : P ratio in pore water (Fig. 8) from above to below the Redfield ratio. This suggests that rates of DIN and DIP efflux from sediments would promote P limitation in the fresh-oligohaline waters and N limitation in mesohaline water. DIP efflux from fresh-oligohaline sediments near sites 1 and 2 may also be restricted because of the pore-water Fe : P ratios being >2, high enough to block PO_4^{3-} efflux by precipitating iron oxyhydroxide P (Lehtoranta and Heiskanen 2003).

Status and implications of the iron conveyer belt hypothesis—Our observations are consistent with the iron conveyer belt hypothesis that PO_4^{3-} is carried from the watershed bound to Fe(III) oxyhydroxides on suspended particles, which are deposited in the estuary and release PO_4^{3-} after reaching saline sediments where sulfides reduce the Fe(III), precipitate Fe(II), and thereby allow the dissolved PO_4^{3-} to diffuse into overlying water. We found that Fe-P concentrations on TSS from the watershed were similar to Fe-P concentrations in sediments deposited near the freshwater end of the estuary. Sediment Fe-P concentration declined with increasing salinity along the estuary, while pore-water PO_4^{3-} concentration increased, suggesting that Fe-P is gradually dissolved in saline sediments. The concentration of dissolved iron in pore water declines sharply as soon as salinity begins to increase. Even at site 2, where pore-water salinity is <2, dissolved iron concentrations are much lower than in the freshwater sediments. Thus, the presence of small amounts of sulfide is apparently sufficient to precipitate much of the iron. Decreases in Fe-P with depth in sediment, from resuspended surface sediments collected in sediment traps down to sediments at 9–11 cm, suggest that the Fe-P dissolution proceeds during early diagenesis and is enhanced at depths where sulfide production takes place.

Although our observations are consistent with the iron conveyer belt hypothesis, it is possible that other factors contribute to the spatial patterns we observed along the salinity gradient. Experiments manipulating salts or sulfate are needed to test the hypothetical causes of the spatial patterns. Indeed, results of experiments adding saltwater to freshwater sediments (Roden and Edmonds 1997; Weston et al. 2006) or adding salts and sulfate to wetland sediments (Beltman et al. 2000; Lamers et al. 2001) support our hypothesized P, Fe, and S interactions.

Unloading PO_4^{3-} from the iron conveyer belt could significantly enhance the input of dissolved PO_4^{3-} to the Patuxent River estuary. The decline in Fe-P from 45 to 20 μmol g^{-1} and the increase in sorb-P from 0.5 to 2.5 μmol g^{-1} as salinity increased along the gradient (Fig. 4) suggest a net unloading of 23 μmol PO_4^{3-} g^{-1}. Multiplying this by the watershed discharge of TSS, 8.1×10^7 kg yr^{-1} (total water flow × flow-weighted mean concentration of TSS; Jordan et al. 2003), suggests that 5.8×10^4 kg PO_4^{3-}-P yr^{-1} could be unloaded from the TSS entering the estuary.

We can also estimate the unloading rate from the watershed discharge of particulate inorganic P (PIP) and the percentage of PIP that is unloaded. As noted above, the net decline in sediment PIP suggests that 23 μmol PO_4^{3-} g^{-1} are unloaded from sediments along the salinity gradient. This is 42% of the PIP concentration in watershed

TSS, which averages 55 μmol g^{-1} (Table 2). Multiplying this percentage by the watershed discharge of PIP, 1.25×10^5 kg yr^{-1} (85% of the total non-point-source PO_4^{3-} discharge; Jordan et al. 2003), suggests an unloading rate of 5.2×10^4 kg PO_4^{3-}-P yr^{-1}, which is very similar to the rate estimated above from TSS discharge. Both estimates assume that all the PIP discharged from the watershed releases an amount of PO_4^{3-} equivalent to the net decrease in concentration of PIP in sediments along the entire salinity gradient we studied. This will produce an overestimate because some of the particulate matter discharged from the watershed accumulates in freshwater sediments where the PO_4^{3-} is retained.

Despite the uncertainty of our estimates, it is clear that unloading the iron conveyer belt could have an important effect on dissolved PO_4^{3-} supply to the estuary. Non-point source discharge of dissolved PO_4^{3-} is 15% of total PO_4^{3-} or 2.2×10^4 kg PO_4^{3-}-P yr^{-1} (Jordan et al. 2003), which less than half of our estimated PO_4^{3-} unloading rates. Point-source PO_4^{3-} discharge is essentially all in dissolved form and equals 3.1×10^4 kg PO_4^{3-}-P yr^{-1} (Jordan et al. 2003), which is 53–60% of our estimated PO_4^{3-} unloading rates.

Our Fe-P unloading estimates are annual rates, but P processing varies with time. PP from the watershed is delivered to the estuary during pulses of high runoff lasting hours or days (Jordan et al. 2003). After delivery, this PP may remain mobile because of the tidal resuspension of surface sediments, as shown by our sediment trap measurements (J. Anderson unpubl. data). Unloading of Fe-P does not seem to occur in pulses related to watershed input. Instead, the summer peaks in PO_4^{3-} release from Patuxent sediments (Boynton et al. 1995) and in the concentration of PO_4^{3-} in overlying water (Fisher et al. 1999) suggest that unloading rates are highest in summer, when rates of SO_4^{2-} and Fe(III) reduction are likely to be highest.

At time scales of years or decades, PP processing is influenced by sediment accretion. Measurements of accretion in the freshwater portion of the Patuxent River estuary indicate that material at 10 cm below the sediment surface, the maximum depth we analyzed, was deposited about 20 yr before present (Khan and Brush 1994). There was a greater decrease in sediment Fe-P along the salinity gradient than with depth down to 10 cm at most locations (Fig. 4). This suggests that Fe-P unloading occurs near the surface, but deep enough for sulfides to be present, possibly within 1 yr or a few years of delivery to the estuary. At 10 cm, the Fe-P concentration at the saline end of our gradient remains about half that of TSS from the watershed. Ongoing deeper sampling (J. Hartzell unpubl. data) will reveal whether this remaining Fe-P is unloaded more than 20 yr after deposition.

The release of PO_4^{3-} from Fe-P contributes to the shift in the pore-water DIN : DIP ratio from much higher than the Redfield ratio in fresh-oligohaline sediments to much lower in more saline sediments (Fig. 8). Thus, unloading the iron conveyer belt may partly account for the generally observed differences in nutrient limitation in freshwater and saltwater. Understanding the effects of PP inputs to a broad range of estuaries requires knowledge the forms and fate of the PP.

Transport and release of PO_4^{3-} by the iron conveyer belt is likely to be especially important in the Patuxent estuary because Fe-P is present at exceptionally high concentration and makes up exceptionally high proportions of the total PP. Estuaries probably differ greatly in the relative importance of different PP fractions and the processes that control the release of PO_4^{3-} from terrigenous PP or the burial of PP. Such differences may reflect differences in surface geology that influence the composition of PP discharged by watersheds. Studies of PP processing in a variety of estuaries will therefore be needed to understand the delivery of P to the world's oceans.

References

Beltman, B., T. G. Rouwenhorst, M. B. Van Kerkhoven, T. Van Der Krift, and J. T. A. Verhoeven. 2000. Internal eutrophication in peat soils through competition between chloride and sulphate with phosphate for binding sites. Biogeochemistry **50:** 183–194.

Berner, R. A., and J. -. L. Rao. 1994. Phosphorus in sediments of the Amazon River and estuary: Implications for the global flux of phosphorus to the sea. Geochim. Cosmochim. Acta **58:** 2333–2339.

———, K. C. Ruttenberg, E. D. Ingall, and J.-L. Rao. 1993. The nature of phosphorus burial in modern marine sediments, p. 365–378. *In* R. Wollast, F. T. Mackenzie and L. Chou [eds.], Interactions of C, N, P and S biogeochemical cycles and global change. NATO ASI Series. Springer-Verlag.

Blomqvist, S., A. Gunnars, and R. Elmgren. 2004. Why the limiting nutrient differs between temperate coastal seas and freshwater lakes: A matter of salt. Limnol. Oceanogr. **49:** 2236–2241.

Boynton, W. R. 2000. Impact of nutrient inflows on Chesapeake Bay, p. 23–40. *In* A. N. Sharpley [ed.], Agriculture and phosphorus management: The Chesapeake Bay. Lewis.

———, J. H. Garber, R. Summers, and W. M. Kemp. 1995. Inputs, transformations, and transport of nitrogen and phosphorus in Chesapeake Bay and selected tributaries. Estuaries **18:** 285–314.

Caraco, N., J. Cole, and G. E. Likens. 1990. A comparison of phosphorus immobilization in sediments of freshwater and coastal marine systems. Biogeochemistry **9:** 277–290.

Cha, H. J., C. B. Lee, B. S. Kim, M. S. Choi, and K. C. Ruttenberg. 2005. Early diagenetic redistribution and burial of phosphorus in the sediments of the southwestern East Sea (Japan Sea). Mar. Geol. **216:** 127–143.

Chambers, R. M., J. W. Fourqurean, J. T. Hollibaugh, and S. M. Vink. 1995. Importance of terrestrially-derived, particulate phosphorus to phosphorus dynamics in a west coast estuary. Estuaries **18:** 518–526.

Cloern, J. E. 2001. Our evolving conceptual model of the coastal eutrophication problem. Mar. Ecol. Prog. Ser. **210:** 223–253.

Coelho, J. P., M. R. Flindt, H. S. Jensen, A. I. Lillebo, and M. A. Pardal. 2004. Phosphorus speciation and availability in intertidal sediments of a temperate estuary: Relation to eutrophication and annual P-fluxes. Estuar. Coastal Shelf Sci. **61:** 583–590.

Compton, J., D. Mallinson, C. R. Glenn, G. Filippelli, K. Föllmi, G. Shields, and Y. Zanin. 2000. Variations in the global phosphorus cycle. Marine authigenesis: From global to microbial, SEPM (Society for Sedimentary Geology) Special Publication **66:** 21–33.

Correll, D. L., T. E. Jordan, and D. E. Weller. 1999. Transport of nitrogen and phosphorus from Rhode River watersheds during storm events. Water Resour. Res. **35:** 2513–2521.

De Jonge, V. N., and L. A. Villerius. 1989. Possible role of carbonate dissolution in estuarine phosphate dynamics. Limnol. Oceanogr. **34:** 332–340.

Environmental Protection Agency—Environmental Monitoring and Assessment Program (EPA-EMAP). 1994. Chesapeake Bay watershed pilot project, EPA/620/R94/020.EPA-EMAP.

Faul, K. L., A. Paytan, and M. L. Delaney. 2005. Phosphorus distribution in sinking oceanic particulate matter. Mar. Chem. **97:** 307–333.

Filippelli, G. M., and M. L. Delaney. 1996. Phosphorus geochemistry of equatorial Pacific sediments. Geochim. Cosmochim. Acta **60:** 1479–1495.

Fisher, T. R., J. D. Hagy, III, W. R. Boynton, and M. R. Williams. 2006. Cultural eutrophication in the Choptank and Patuxent estuaries of Chesapeake Bay. Limnol. Oceanogr. **51:** 435–447.

———, and others. 1999. Spatial and temporal variation of resource limitation in Chesapeake Bay. Mar. Biol. **133:** 763–778.

Föllmi, K. B. 1996. The phosphorus cycle, phosphogenesis and marine phosphate-rich deposits. Earth Sci. Rev. **40:** 55–124.

Gächter, R., and B. Müller. 2003. Why the phosphorus retention of lakes does not necessarily depend on the oxygen support to their sediment surface. Limnol. Oceanogr. Notes **48:** 929–933.

Howarth, R. W., and R. Marino. 2006. Nitrogen as the limiting nutrient for eutrophication in coastal marine ecosystems: Evolving views over three decades. Limnol. Oceanogr. **51:** 364–376.

Hyacinthe, C., and P. Van Cappellen. 2004. An authigenic iron phosphate phase in estuarine sediments: Composition, formation and chemical reactivity. Mar. Chem. **91:** 227–251.

Jensen, H. S., P. B. Mortensen, F. O. Andersen, and A. Jensen. 1995. Phosphorus cycling in a coastal marine sediment, Aarhus Bay, Denmark. Limnol. Oceanogr. **40:** 908–917.

———, and B. Thamdrup. 1993. Iron-bound phosphorus in marine sediments as measured by bicarbonate-dithionite extraction. Hydrobiologia **253:** 47–59.

Jordan, T. E., D. L. Correll, J. Miklas, and D. E. Weller. 1991. Nutrients and chlorophyll at the interface of a watershed and an estuary. Limnol. Oceanogr. **36:** 251–267.

———, D. E. Weller, and D. L. Correll. 2003. Sources of nutrient inputs to the Patuxent River estuary. Estuaries **26:** 226–243.

Khan, H., and G. S. Brush. 1994. Nutrient and metal accumulation in a freshwater tidal marsh. Estuaries **17:** 345–360.

Lamers, L. P. M., G. Els Ten Dolle, S. T. G. Van Den Berg, S. P. J. Van Delft, and J. G. M. Roelofs. 2001. Differential responses of freshwater wetland soils to sulphate pollution. Biogeochemistry **55:** 87–101.

Lebo, M. E., and J. H. Sharp. 1993. Distribution of phosphorus along the Delaware, an urbanized coastal plain estuary. Estuaries **16:** 290–301.

Lehtoranta, J., and A.-S. Heiskanen. 2003. Dissolved iron:phosphate ratio as an indicator of phosphate release to oxic water of the inner and outer coastal Baltic Sea. Hydrobiologia **492:** 69–84.

Liu, S. M., J. Zhang, and D. J. Li. 2004. Phosphorus cycling in sediments of the Bohai and Yellow Seas. Estuar. Coastal Shelf Sci. **59:** 209–218.

Louchouarn, P., M. Lucotte, E. Duchemin, and A. De Vernal. 1997. Early diagenetic processes in recent sediments of the Gulf of St-Lawrence: Phosphorus, carbon and iron burial rates. Mar. Geol. **139:** 181–200.

Lung, W.-S., and S. Bai. 2003. A water quality model for the Patuxent Estuary: Current conditions and predictions under changing land-use scenarios. Estuaries **26:** 267–279.

Nilsen, E. B., and M. L. Delaney. 2005. Factors influencing the biogeochemistry of sedimentary carbon and phosphorus in the Sacramento-San Joaquin Delta. Estuaries **28:** 653–663.

Pacini, N., and R. Gächter. 1999. Speciation of riverine particulate phosphorus during rain events. Biogeochemistry **47:** 87–109.

Paludan, C., and J. T. Morris. 1999. Distribution and speciation of phosphorus along a salinity gradient in intertidal marsh sediments. Biogeochemistry **45:** 197–221.

Parsons, T. R., Y. Maita, and C. M. Lalli. 1984. A manual of chemical and biological methods for seawater analysis, 1st ed. Pergamon.

Pionke, H. B., and H. M. Kunishi. 1992. Phosphorus status and content of suspended sediment in a Pennsylvania watershed. Soil Sci. **153:** 452–462.

Roden, E. E., and J. W. Edmonds. 1997. Phosphate mobilization in iron-rich anaerobic sediments: Microbial Fe(III) oxide reduction versus iron-sulfide formation. Arch. Hydrobiol. **139:** 347–378.

Ruttenberg, K. C. 1992. Development of a sequential extraction method for different forms of phosphorus in marine sediments. Limnol. Oceanogr. **37:** 1460–1482.

———, and R. A. Berner. 1993. Authigenic apatite formation and burial in sediments from non-upwelling, continental margin environments. Geochim. Cosmochim. Acta **57:** 991–1007.

Seitzinger, S. P. 1991. The effect of pH on the release of phosphorus from Potomac Estuary sediments: Implications for blue-green algal blooms. Estuar. Coastal Shelf Sci. **33:** 409–418.

Slomp, C. P., E. H. G. Epping, W. Helder, and W. V. Raaphorst. 1996. A key role for iron-bound phosphorus in authigenic apatite formation in North Atlantic continental platform sediments. J. Mar. Res. **54:** 1179–1205.

Sprugel, D. G. 1983. Correcting for bias in log-transformed allometric equations. Ecology **64:** 209–210.

Strom, R. N., and R. B. Biggs. 1982. Phosphorus distribution in sediments of the Delaware River Estuary. Estuaries **5:** 95–101.

Subramanian, V. 2000. Transfer of phosphorus from the Indian sub-continent to the adjacent oceans. Marine authigenesis: From global to microbial, SEPM (Society for Sedimentary Geology) Special Publication **66:** 77–88.

Sundareshwar, P. V., and J. T. Morris. 1999. Phosphorus sorption characteristics of intertidal marsh sediments along and estuarine salinity gradient. Limnol. Oceanogr. **44:** 1693–1701.

Tamburini, F., S. Huon, P. Steinmann, F. E. Grousset, T. Adatte, and K. B. Fllmi. 2002. Dysaerobic conditions during Heinrich events 4 and 5: Evidence from phosphorus distribution in a North Atlantic deep-sea core. Geochim. Cosmochim. Acta **66:** 4069–4083.

Tyrrell, T. 1999. The relative influences of nitrogen and phosphorus on oceanic primary production. Nature **400:** 525–531.

Upchurch, J. B., J. K. Edzwald, and C. R. O'Melia. 1974. Phosphates in sediments of Pamlico Estuary. Environ. Sci. Technol. **8:** 56–63.

Van Der Zee, C., C. P. Slomp, and W. Van Raaphorst. 2002. Authigenic P formation and reactive P burial in sediments of the Nazare canyon on the Iberian margin (NE Atlantic). Mar. Geol. **185:** 379–392.

Virtasalo, J. J., T. Kohonen, I. Vuorinen, and T. Huttula. 2005. Sea bottom anoxia in the Archipelago Sea, northern Baltic Sea—implications for phosphorus remineralization at the sediment surface. Mar. Geol. **224:** 103–122.

Weston, N. B., R. E. Dixon, and S. B. Joye. 2006. Ramifications of increased salinity in tidal freshwater sediments: Geochemistry and microbial pathways of organic matter mineralization. J. Geophys. Res. **111**, G01009, doi:01010.01029/02005JG000071.

Wu, J., W. Sunda, E. A. Boyle, and D. M. Karl. 2000. Phosphate depletion in the western North Atlantic Ocean. Science **289:** 759–762.

Received: 29 November 2006
Accepted: 18 June 2007
Amended: 13 August 2007